In Situ Surface Enhanced Infrared Absorption Spectroscopy Study of the Adsorption of Cytosine on Gold Electrodes.

Julia Alvarez-Malmagro, Francisco Prieto* and Manuela Rueda

Department of Physical Chemistry, Phaculty of Chemistry, University of Seville, c/ Prof. Garcia Gonzalez 1, 41012, Sevilla, SPAIN

*E-mail: dapena@us.es

Dedicated to Professor Claudine Buess-Hermann for her relevant contributions to Electrochemistry.

Abstract

The structural facilities provided by the 'in situ' Surface-Enhanced Infrared Absorption Spectroscopy in the Attenuated Total Reflection mode (ATR-SEIRAS) are exploited for the characterization of cytosine adsorption on gold thin-film electrodes from acid, neutral and basic solutions, using H_2O and D_2O as solvents. The experimental conditions are selected in order to consider the two forms involved in the first acid-base equilibrium and in the tautomeric keto-enol and amino-imino equilibria of the molecule. The results are compared with the corresponding absorption FT-IR spectra of cytosine in solution. DFT calculations are used to optimize the molecular geometries and to estimate the vibrational properties of the different acid-base and tautomeric forms, either in solution or in the adsorbed state on gold surfaces.

The comparison between the spectra in solution and in the adsorbed state indicates the adsorption of the deprotonated form even at pH bellow the first pK_a of cytosine. Therefore, only the tautomeric forms of the deprotonated cytosine are considered: the keto-amino (*C1* and *C4*), the enol-amino (*C2*) and the keto-imino (*C3*) tautomers of cytosine and of deuterated cytosine molecules.

Interpretations of the absorption FT-IR spectra of the molecules in solution based on DFT calculations suggest the preponderance of the *C1* tautomer in solution but with contributions of the *C3* tautomer, in neutral and basic media. However, the interpretations of the ATR-SEIRAS experiments show the preponderance of tautomer *C3* in the adsorbed state with contributions of tautomer *C1* depending not only on the pH of the solution, but also on the potential applied to the electrode.

1.- INTRODUCTION

Cytosine as one of the DNA bases plays an important role in genetic expression and replication. These phenomena are linked to cytosine base pairing with its complementary base, guanine, that in the double helix takes place by three H-bonds involving the oxygen of the keto group and the hydrogen atoms connected to the amino and the intra-cyclic nitrogen atoms, of the more stable canonical keto-amino tautomers[1] (see Scheme 1). However, the suggestion by Watson and Crick that "rare" tautomers may be responsible for genetic errors, via base mispairing, impulse the investigation about DNA bases tautomerism by different experimental and theoretical methodologies.[2–22] The appearance of less stable non-canonical tautomeric forms of DNA can be due to external environmental parameters or to structural modifications such as methylation, and also by proton transfer in the inter-base hydrogen bonds during replication that trigger the spontaneous mutation, thus causing errors in the transmission of DNA sequences.[23–25]

The enol-amino and the keto-imino tautomers were detected for methylated cytosine derivatives in the gas phase or in low-temperature matrices as well as in solution.[26–29] Even for unsubstituted cytosine, the canonical keto-amino form with the H atom in the N1 position undergoes interconversion to the tautomer with the H atom in the N3 position in aqueous solutions, depending on the pH value.[27] The cytosine-guanine tautomerism was recently reviewed by Brovarets et al.[11]

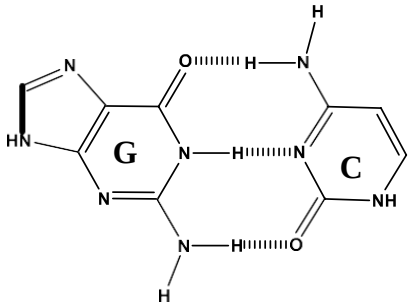

Scheme 1. Watson and Crick (WC) interaction between Cytosine and guanine.

Among the experimental methods to study base paring interactions, those involving the adsorption of the bases on solid substrates are specially interesting nowadays for fundamental and practical reasons. From the fundamental point of view it can be

mentioned the relevance of the structural information that methods such as scanning probe microscopy[30], surface-enhanced Raman scattering (SERS)[31] or surface-enhanced infrared absorption spectroscopy (SEIRAS)[32], among others, can provide about the intermolecular interactions of adsorbates on solid surfaces. The electrochemical methods, in combination with the nanoscopic or vibrational spectroscopies have, in addition, the feasibility to study the influence of electric fields of similar intensities to those existing in biological interfaces where the bases pairing interactions occur[33]

On the other hand, the adsorption of DNA bases on solid substrates has important practical implications in the manufacturing of biosensors for DNA sequencing recognition,[34] in targeted drug delivery[34] or in molecular electronic nanotechnologies.[35–37]. Wandlowski et al.[38] studied the electrochemical adsorption of cytosine on Au (111) electrodes from aqueous solutions by electrochemical methods and scanning tunnelling microscopy (STM) under potential control, and distinguished different potential regions starting from negative potentials, at which cytosine forms a disordered phase of weakly adsorbed molecules, to the most positive potentials at which a chemically bounded cytosine adlayer is formed. The authors proposed a vertical molecular orientation on the electrode surface, with coordination to gold atoms via the N3 position. On the contrary, Tao et al.[39], who also used electrochemical and STM methods to study cytosine adsorption on Au(111) electrodes, proposed a flat lying molecules orientation on the gold surface. Ataka et al.[32] used cytosine adsorption on gold thin-layer film electrodes to reveal the interesting possibilities of SEIRAS in the Kretschmann attenuated-total-reflection (ATR) configuration. They also found different adsorption states depending on the electrode potential, that they interpreted as physically or chemically adsorbed cytosine films, formed by more or less perpendicular cytosine molecules that provides surface-active IR spectral signals.

Recently, the interest to model DNA bases adsorption on Au(111) surfaces by DFT calculations is increasing as the corresponding methodology is developing to allow its application to complex biomolecules[13,40,41]

The authors have been studying the electrochemical adsorption of the complementary DNA bases adenine and thymine by modern in-situ FTIR techniques and have provided detailed information about their different acid-base and tautomeric forms.[42–47] It was

found that the two complementary bases get deprotonated in order to chemically coordinate to the gold surface, even at pH values several units lower than their first pK_a. In the case of thymine adsorption,[47] the preponderance of the tautomers deprotonated in the nitrogen atoms N1 or N3 of the molecule was inferred from the IR spectra when compared with the DFT calculated spectra for the two tautomers. It was found that the N3 tautomer is the predominant adsorbed species in the experiments in acid media while the adsorbed N1 tautomer predominates in the case of the adsorption from basic media solution. In addition, it was concluded that each tautomer undergoes different molecular reorientations with the electric field applied to the electrode.

In this paper, the high sensitivity and its facility to correct the interferences from the bulk solution of the ATR-SEIRAS in the Kretschmann configuration technique are exploited to study cytosine adsorption on gold thin film electrodes, from aqueous solutions at three pH values, in order to determine the adsorption behavior of the different forms that are connected to acid-base or tautomeric equilibria. Cytosine molecule in aqueous solutions is involved in two acid-base equilibria with pKa values of 4.5 and 12.2[48] (see Scheme 2). Electrochemical and spectroscopic experiments have been performed at three pH values corresponding to acid medium in which the protonated molecule is present in solution, and to neutral and basic media below the second pK_a value, so the anionic cytosine molecule has a low contribution to the solution composition.

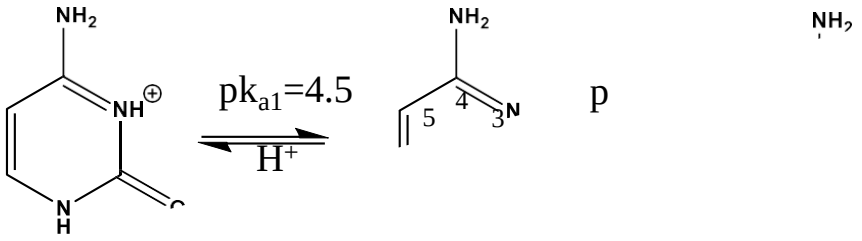

Scheme 2. Cytosine acid-base equilibria.

The spectroscopic results have been compared with the DFT calculated spectra of different adsorbed cytosine tautomers over gold clusters, for their interpretation. In Scheme 3, the tautomers that are considered in the paper are formulated. These are the canonical keto-amine tautomer with the nitrogen N1 protonated (*C1*), the enol.amine tautomer (*C2),* the keto-imine tautomer *(C3*) and the keto-amine tautomer with nitrogen N3 protonated (*C4*). The interpretations of the spectra are mainly based on the signals

associated to vibrations of the carbonyl and amino moieties of the molecules appearing in the 1300 to 1800 cm^{-1} spectral region. The signals assigned to the amino group bending mode, however, shift to the red upon deuteration, thus facilitating the interpretation of spectra in this frequency region. Therefore, experiments have also been performed in deuterated media and the DFT spectra for the four adsorbed deuterated tautomers have also been calculated. Experimental and theoretical spectra of the species in solution have also been obtained for comparison with the adsorbed cytosine species

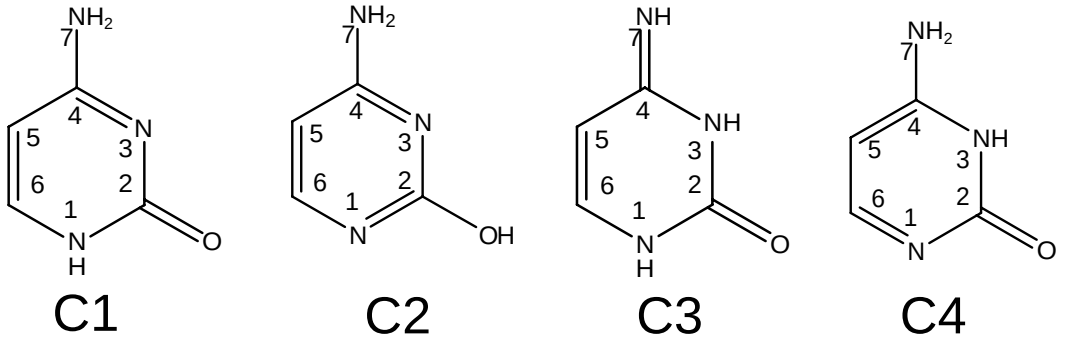

Scheme 3. Tautomeric forms of cytosine.

2.- EXPERIMENTAL

2.1.- Reagents and solutions.

Working solutions for the electrochemical and spectroelectrochemical experiments were prepared by dosing the required volume of 10 mM stock solution of cytosine (Sigma-Aldrich, as received) over controlled volumes of supporting electrolyte solutions to get a final concentration 1mM. The supporting electrolyte solutions consisted in 0.1 M $HClO_4$ (pH 1), 0.1 M $KClO_4$ (pH 7), 0.1 M NaF (pH 8) or 0.1 M $KClO_4$ + NaOH (pH 11) in ultrapure H_2O (Milli-Q, Millipore) or in D_2O (99.5%, Sigma-Aldrich). All the reagents for the supporting electrolyte were suprapure grade (Merck).

All the glassware was cleaned by overnight immersion in an acid solution of K_2MnO_4, washed afterwards with dilute piranha solution and thoughtfully rinsed with ultrapure water.

2.2.-Electrochemical measurements.

A 50 mL glass electrochemical cell with three electrodes configuration was used. A gold wire, freshly purified by flame annealing, was the counter electrode. The reference electrode was a $K_2SO_{4(sat)}|Hg_2SO_{4(s)}|Hg_{(l)}$ electrode connected to the cell by an intercalated salt-bridge filled with the same supporting electrolyte. All the potentials are referred to the saturated calomel electrode (SCE). The working electrode consisted in a freshly flame annealed[49] gold single crystal prepared according to Clavilier method[50], with a (111) orientation, contacting the working solution by the meniscus method.

Prior to any electrochemical measurements, oxygen in solutions was eliminated by bubbling argon during 20 minutes. A flow of the inert gas was kept over the working solution during the measurements.

Cyclic voltammograms were obtained with an Ivium Stat from IVIUM multimode electrochemical instrument at a scan rate of 50 mV s^{-1}.

2.3.- FT-IR spectroscopy experiments.

'In situ' ATR-SEIRAS measurements were performed with a set up based on the Kretschmann configuration for internal reflection, using a borosilicate spectroelectrochemical cell filled with 15 mL of working solution. The IR window, at the bottom of the cell, was a silicon prism beveled at 60 degrees. The working electrode was formed on the upper face of the silicon prism by cathodic deposition of a gold film of thickness 20-25 nm at a deposition rate of c.a. 1 nm min^{-1}, with a Leica EM SCD 500 metalizer, equipped with a crystal microbalance to control the deposition rate and thickness. Under these conditions, the film surface contains predominantly Au(111) domains [51]. Then, the gold nano film electrode was cleaned inside the spectroelectrochemical cell filled with the supporting electrolyte by cycling the potentials of the capacitative region conforming to successive CV perturbations during 60 minutes. Finally, supporting electrolyte was replaced previously to any further experiment. The same reference electrode as in the CV experiments and a gold foil

counter electrode completed the cell. Electrochemical control was exerted by a CH1100 A potentiostat from CH instruments.

Every spectroelectrochemical experiment was initiated by collecting the reflectance spectra at different dc potentials for working solutions containing only the supporting electrolyte. These spectra were used as reference reflectance (R_0). Afterwards, the required volume of cytosine 10 mM stock solution was dosed to the cell to a final 1 mM concentration. The sample reflectance spectra (R) were then collected. The wavenumber precision used was 4 cm^{-1}, and 100 interferograms were averaged for every single reflectance spectrum. The final spectra are represented as log (R_0/R) vs wavenumber.

Absorption spectra of cytosine in solution were obtained in two ways:

For D_2O solutions, a dismountable transmission cell from Pike Instruments with two CaF_2 windows and a path length of 51 μm (measured from the interference fringes obtained with the cell filled with air[52]). For H_2O solutions, the same ATR cell used for spectroelectrochemical measurements was employed, but with a 45 degrees ZnSe prismatic optical window in order to attain a better correction of the solvent absorption bands in the region of 1600-1700 cm^{-1}. The background spectra were measured after filling the cell with pure solvent while the sample spectra were collected with 10 mM cytosine solutions in the supporting electrolyte of the desired pH value. The final spectra represent the absorbance (for experiments with the transmission cell) or log (R_0/R) (for experiments with the ATR cell). 1000 interferograms were collected for every single spectrum with a precision of 4 cm^{-1} to obtain the better relation signal/noise.

A Nicolet 6700 FT-IR spectrometer equipped with a MCT-A detector cooled with liquid nitrogen was used for all the spectroscopic measurements.

2.4.- DFT calculations.

Geometry optimizations and vibrational frequency calculations for cytosine tautomers in gas phase have been performed using the hybrid functionals B3LYP and PBE as implemented in the Gaussian'09 package[53], in combination with the 6-311+G(d) basis set[54–56]. The calculations have also been performed considering the effect of the solvent on the isolated molecule by a continuum polarization model (PCM). The

theoretical vibrational frequencies have been corrected by the scaling factors optimized for the functional and basis sets used.[57]

For calculations with adsorbed cytosine Au(111) surfaces, a layer of 19 atoms of gold with a fixed geometry was used. The B3LYP functional and the 6-311+G(d) basis sets for C, N, O and H atoms and the pseudopotential LANDL2DZ[58] basis set for Au atoms were employed. The geometrical optimization of the system allowed the free movement of the coordinates of the nucleobase. Different starting geometries were employed to discard the possibility of local minima or border effects. Although this model with a single gold atoms layer is less exact in terms of adsorption energies than a cluster model with more gold layers or a slab model because of the electronic delocalization in metallic systems, it must provide good values of local properties like the vibrational frequencies, target of these calculations. The same cluster model, functional, basis sets and pseudopotential and procedures were used in a previous work about the adsorption of thymine on gold electrodes, providing an excellent agreement between the theoretical and experimental IR spectra. [47]

3.- RESULTS AND DISCUSSION

3.1.- Cyclic voltammetry.

Fig. 1 shows the cyclic voltammograms registered with cytosine containing solutions at three different pH values. Four potential regions can be differentiated on neutral and basic pHs, exhibiting a behavior similar to the one of thymine adsorbed on Au(111) electrodes[47,59]. Regions I and II are delimited by a couple of broad and low peaks. Region III correspond to highly asymmetric chemical adsorption/desorption peaks. As previously proposed by Wandlowski et al[38], regions I and II could correspond to the physisorption of cytosine with two different organizations. Region IV corresponds to a compact layer of chemisorbed cytosine.

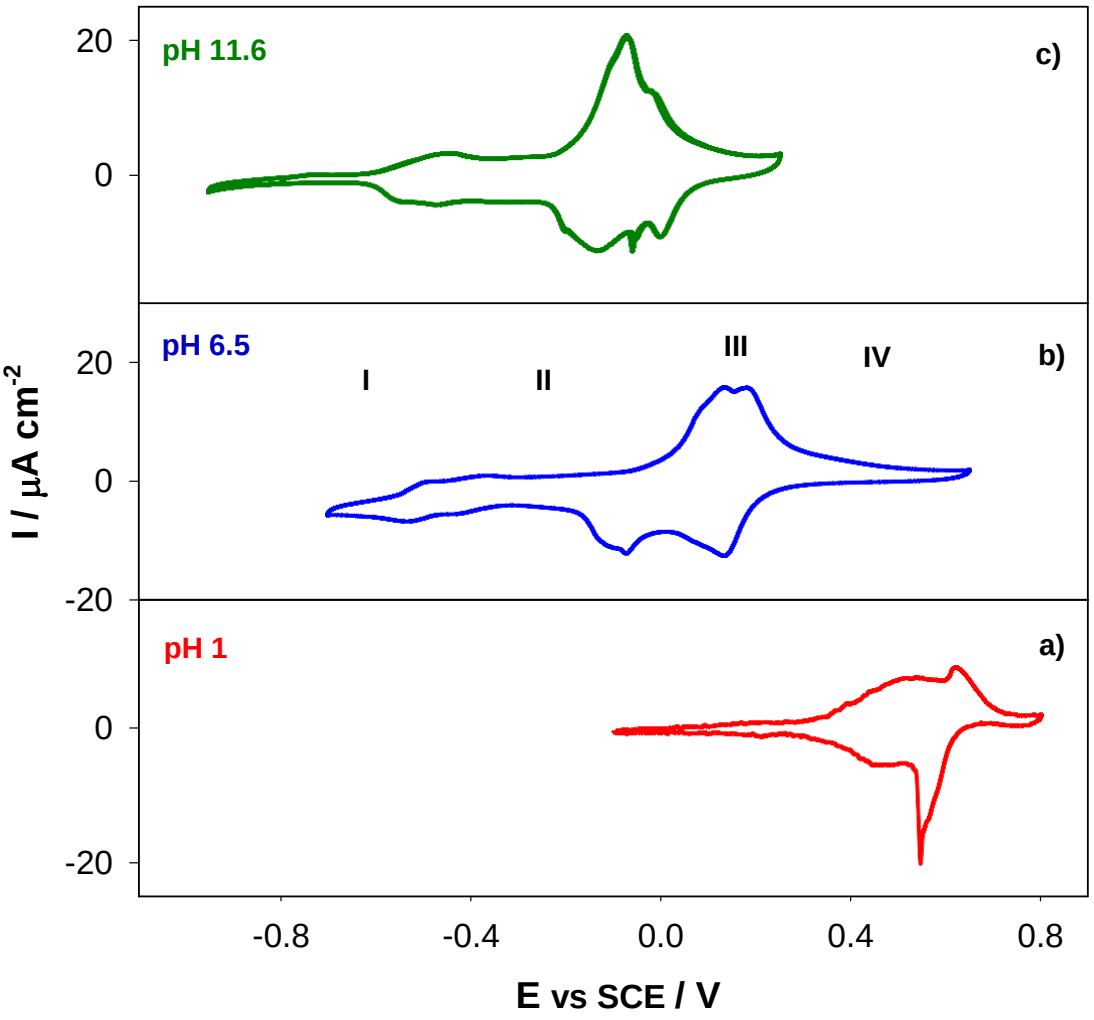

Figure 1.- Cyclic voltammograms obtained at 50 mV s^{-1} with an Au(111) electrode in cytosine containing solutions at pH 1 and cytosine 1 mM a), pH 6.5 and cytosine 1 mM b) and pH 11.5 and cytosine 0.1 mM c).

The potential ranges corresponding to the four regions are roughly similar at pH 6.5 and pH 11.5, although the shape of the peaks in region III changes between both pH values. On the contrary, at pH values lower than the first pK_a of cytosine, the potential regions II and III and IV are clearly shifted towards higher potentials. This potential shift with the pH can be explained if the adsorption of cytosine from acid solutions ($pH < pK_{a1}$) involves the deprotonation of the cationic protonated cytosine that is present in solution. On the other hand, the asymmetry in the adsorption/desorption peaks in region III suggests the existence of kinetic effects in the chemical adsorption process. The study by chronoamperometry of the dissolution of the adlayer in region IV[38] indicated that the chemical desorption process is a combination of a Langmuir type desorption and a hole-nucleation and growth dissolution mechanism.

3.2.- FT-IR spectroscopy of cytosine in solution.

The absorption FT-IR spectra in the 1800-1350 cm^{-1} region of cytosine in solution, which contains the most significant features, are shown in Figs. 2a and 3a for D_2O and H_2O solutions, respectively. The spectra of cytosine (Cyt-h3) in H_2O solutions at pH values 7 and 11.5 in Fig. 3a can be considered coincident, as can be expected if the same species is present in solution at both pHs values, with two overlapped broad bands at 1635 cm^{-1} and 1675 cm^{-1}, and some other minor signals at lower wavenumbers. The spectrum of cytosine (Cyt-d3) in neutral D_2O solutions, in Fig. 2a, has different features as a consequence of the isotopic change of the amine hydrogen atoms that shifts the NH_2 and NH bending modes towards lower wavenumbers. A single intense band is obtained at c.a. 1640 cm^{-1}, that must correspond to carbonyl group stretching vibration and four medium or intense bands at c.a. 1600, 1580, 1512 and 1500 cm^{-1} that must include ring CC and CN stretching vibrations. At pH or pD 1, the absorption spectral bands of cytosine in solution shift to higher wavenumber, as a consequence of the protonation of the molecule, as was found for adenine at pH values lower than its first pKa (4.5)[44]. As cyclic voltammetry suggests and as the spectroelectrochemical results show (see next section), the protonated cytosine does not adsorb on the gold electrode even from solutions at pH 1, and only the neutral unprotonated species does. Therefore, the discussion will be focused on the neutral cytosine spectra.

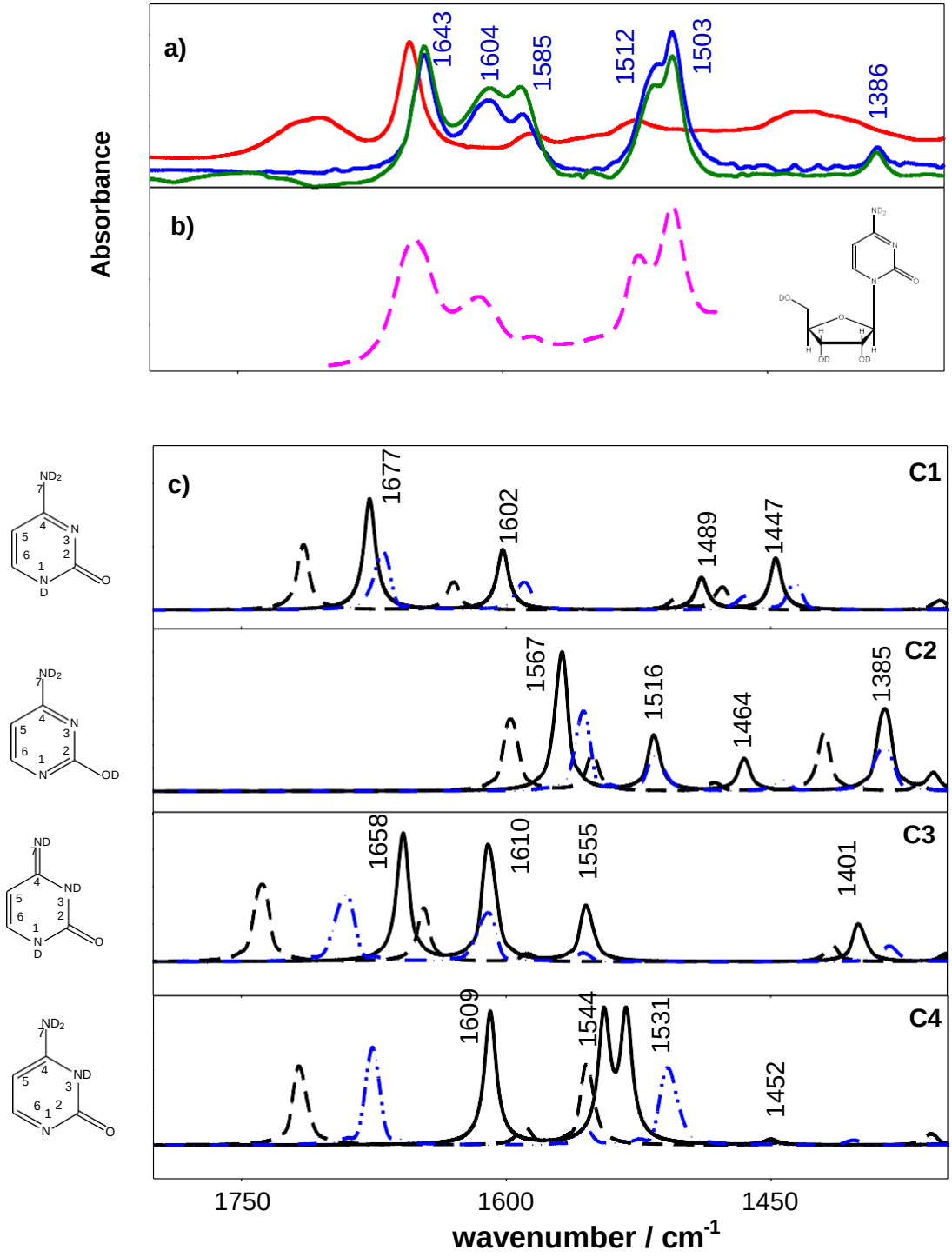

Figure 2.- Absorption FT-IR spectra in the 1800-1350 cm^{-1} region of a) Cyt-d3 in D_2O solutions at pD 1 (red line), pD 7 (blue line) and pD 11 (green line) and of b) Cytidine in neutral D_2O solution (pink line). c) Calculated IR spectra of Cyt-d3 tautomers indicated in the plots using the functionals B3LYP (blue dash-dot-dot line), PBE (black dashed line) and PBE with PCM for the solvent (black solid line).

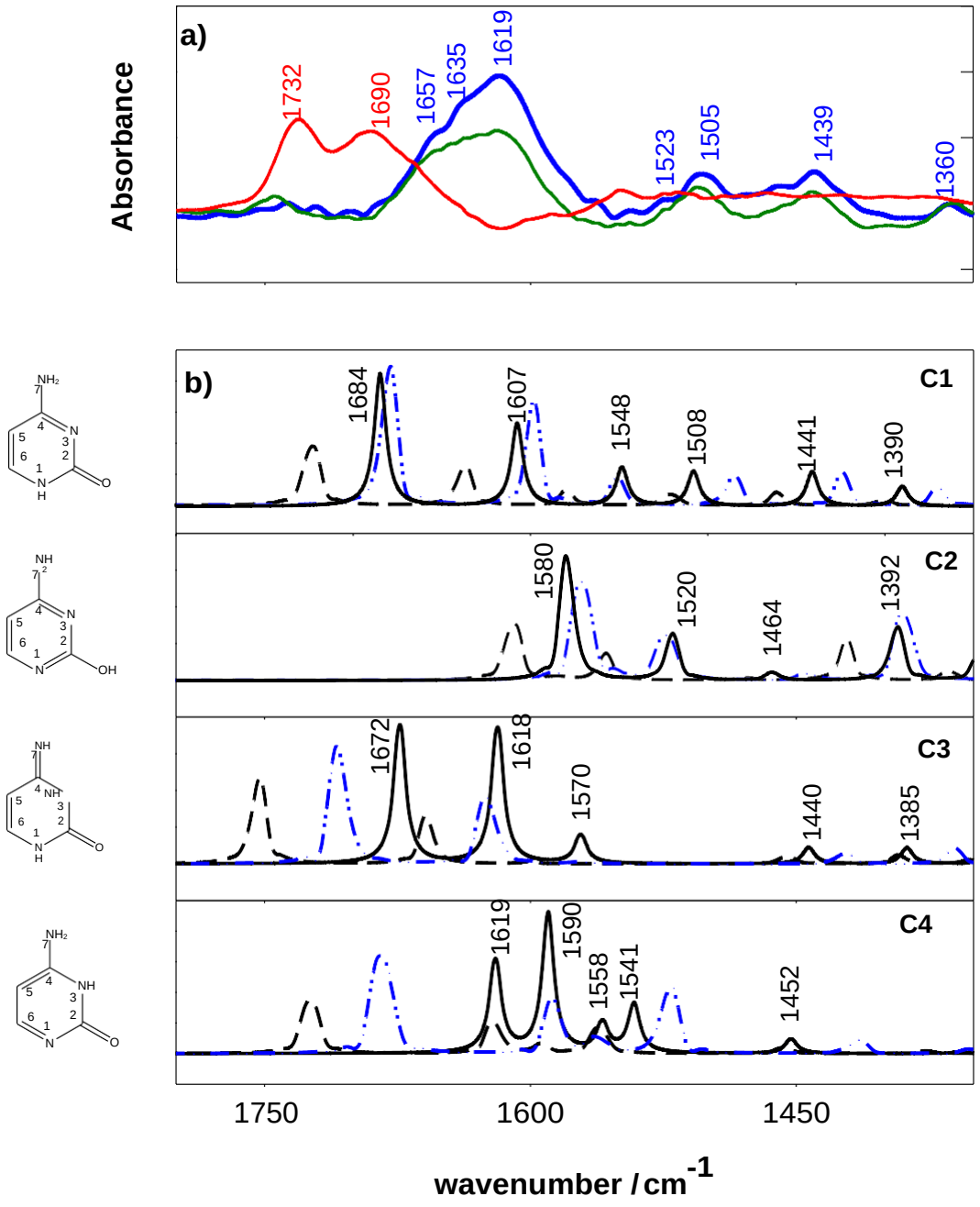

Figure 3.- a) Absorption FT-IR spectra in the 1800-1350 cm^{-1} region of Cyt-h3 in H_2O solutions. at pH 1 (red line), 7 (blue line) and 11.5 (green line). b) DFT calculated IR spectra of Cyt-h3 tautomers indicated in the plots. Lines as in figure 2.

In order to identify the tautomer of cytosine present in solutions at pH 7 and 11.5, DFT geometry optimizations and vibrational spectra simulations have been performed with two different functionals over four tautomeric forms of neutral cytosine: Tautomer *C1* corresponds to the canonical keto-amine form with the hydrogen connected to the N1

atom, *C2* to the amine-enol form; *C3* is the keto-imine tautomer and *C4* is the keto-amine tautomer with hydrogen connected to N3 atom.

Table 1. Relative DFT electronic energies for the optimized geometries of the cytosine tautomers indicated obtained with the B3LYP and PBE functionals and 6-311—(gd) basis sets

Tautomer	E(B3LIP) /eV	E(PBE)/eV	E/(PBE-PCM)/eV
C1	0	0	0
C2	0.04	0.08	0.31
C3	0.07	0.08	0.23
C4	0.31	0.30	0.17

Table 1 contains the electronic energies of the four tautomers relative to the lowest value. Independently of the functional used in the calculations and the consideration of the solvent effects by a polarizable continuum model (PCM), the lowest energy corresponds to the *C1* tautomer, although the relative energies of other tautomers are lower than 0.3 eV. Therefore, and taking into account the limitations of the model used in the calculations, the resultant energies cannot be considered a conclusive sign of the relative stabilities of the four cytosine tautomers in solution.

More evidences of the tautomeric forms existing in solutions can be obtained by comparing the experimental FT-IR spectra of cytosine in solution with the calculated spectra for the different tautomeric forms. In Fig. 2b and 3b the calculated spectra with the B3LYP and the PBE functionals are shown. The different calculation procedures provide similar features, although the positions of the bands depend on the functionals used in the calculations, especially in what concern the signals due to the carbonyl-stretching mode. Particularly, the PBE functional overestimates these frequencies if the solvent is not taken into account at least like a continuum polarizable medium. The experimental and calculated vibrational frequencies obtained with the PBE-PCM model are included in Table S1 and Table S2 in the supporting information. These are very close to the ones obtained with the B3LYP functional.

Independently on the DFT model used, the experimental absorption bands at wavenumbers higher than 1640 cm^{-1}, either in D_2O or in H_2O, involve the stretching mode of the carbonyl group. Therefore, the majoritarian tautomer in solution cannot be the enol-amine form, *C2*.

Focusing on the experimental spectrum of Cyt-d3 in neutral D_2O solutions, the two absorption bands at 1503 cm^{-1} and 1512 cm^{-1} could be initially ascribed to skeletal stretching and CH bending vibrational modes of either *C4* or *C1* tautomers, that present theoretical absorption bands at 1531-1544 cm^{-1} and 1447-1489 cm^{-1}, respectively. To discriminate between both tautomers, the experimental spectrum of cytidine in neutral D_2O solution has been included in Fig. 2b for comparison. Cytidine cannot adopt the *C4* tautomeric form as the N3 atom is bonded to the sugar moieties. However, the spectrum for cytidine in Fig 2b shows the bands at 1503-1512 cm^{-1}, so these two signals have to be ascribed to the *C1* tautomer of cytidine and of cytosine, which must be then the majoritarian tautomer for these molecules in neutral solutions, in view of the high intensity of these signals.

However, the exclusive presence of *C1* tautomer cannot explain the appearance of three absorption bands in the 1580-1680 cm^{-1} range, as only two bands are expected for this tautomer according to DFT calculations (see Fig. 2). Therefore, the existence of more tautomeric forms in solution must be accepted. The signal at 1585 cm^{-1} could match the theoretical ring-stretching (C4C5 and C2N3) vibration modes in *C2* tautomer. However, the experimental spectrum should show more signals in the 1350 to 1550 cm^{-1} range, corresponding to other vibration modes of the *C2* tautomer. On the other hand, *C3* tautomer presents theoretical bands at 1658 cm^{-1} and 1609 cm^{-1}, assigned to CO and C5C6 stretching vibrations, respectively, very close to the corresponding bands in the *C1* tautomer theoretical spectrum (1677 and 1602 cm^{-1}), so both set of bands can overlap into the experimental signals at 1643 and 1604 cm^{-1}. Moreover, the presence of *C3* tautomer would explain the experimental signal at 1585 cm^{-1}, that can be identified with the stretching (C4N7+C4C5) mode at 1553 cm^{-1}.

Therefore, although the contribution of *C2* tautomer cannot be completely discarded, the combination of the canonical *C1* and the keto-imino *C3* tautomer can better explain the experimental spectrum of cytosine in neutral deuterated solutions. This hypothesis can also explain the experimental spectrum of cytosine in neutral H_2O solutions, although the overlapping of the cytosine signals with the solvent IR absorption bands in this region introduces some difficulties in the assignments. The wide and overlapped signals at 1600-1680 cm^{-1} can correspond to the theoretical signals at 1684 and 1607 cm^{-1} (for *C1*) and at 1674 and 1619 (for *C3*). The minor bands at 1498, 1434 and 1359 cm^{-1} are assigned to the theoretical signals for *C1* at 1508, 1434 and 1359 cm^{-1}. The

theoretical signals for the *C3* tautomer in the lower frequency part of the region are very weak and, also because of the low concentration of the tautomer, they are hardly noticed in the experimental spectrum.

3.3.- ATR-SEIRA spectra of cytosine adsorbed on gold electrodes.

3.3.1.- Spectra in the 1800-1350 cm^{-1} region.

Fig. 4 shows the ATR-SEIRA spectra of Cyt-d3 adsorbed on nanostructured gold electrodes from D_2O solutions at three different pDs and at electrode potentials corresponding to the chemisorbed layer (region IV of the voltamograms in Fig. 1). According to the surface reflection rules, the presence of active absorption signals corresponding to the spectral region of in-plane vibrations indicate that cytosine chemisorbs with the molecular plane normal or tilted relative to the electrode surface.

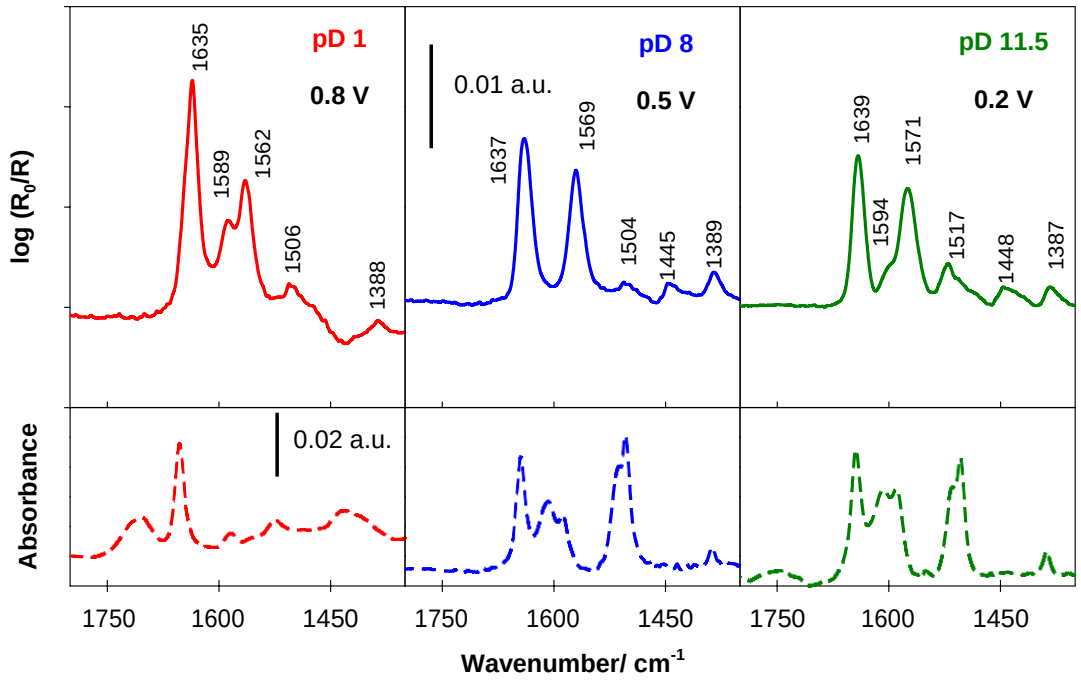

Figure 4.- ATR-SEIRA spectra of cytosine adsorbed on gold electrodes from D_2O solutions at the indicated potentials and pD (solid lines). The absorption spectra of cytosine in solution at the same pD values are included in the lower part of the figure for comparison (dashed lines).

Most of the spectral features observed at the three pD values are coincident: two strong bands at c.a 1637 cm^{-1} and 1569 cm^{-1} and three weak bands at 1504, 1445 and 1389 cm^{-1}, indicating that the same species must be predominant in the chemisorbed state in the whole pH range. The absence of signals at wavenumbers close to 1700 cm^{-1} and the

comparison of the ATR-SEIRA spectra with the absorption spectra in solution, included in the lower part of Fig. 4, allow one to conclude that the chemisorbed cytosine form must be the neutral unprotonated molecule, even at pD 1 at which the predominant form in solution is the cationic protonated form, as inferred from the comparison of the FT-IR spectra in solution at the different pD values (see Fig. 2b). However, it should be noted that the spectra of adsorbed cytosine from the acid and basic solutions in Fig. 4 show a more or less overlapped signal around 1590 cm^{-1}, which could indicate changes in the preponderance of different tautomeric forms with the pD of the solution.

On the other hand, the ATR-SEIRA spectra of chemisorbed Cyt-d3 in Fig. 4 do not seem to be coincident with the FT-IR spectra of Cyt-d3 in solution. For instance, the ATR-SEIRAS do not show any of the two intense bands at 1512 and 1503 cm^{-1} that are present in the FT-IR spectra of Cyt-d3 in solution, assigned to characteristic ring stretching modes of the *C1* tautomer.

In order to explain the spectra in Fig. 4, DFT calculations of the four adsorbed Cyt-d3 tautomer molecules have been performed. As indicated in the experimental section, the model employed was a cluster of 19 gold atoms with the Au(111) geometry. The geometrical optimizations of the four tautomeric forms of Cyt-d3 adsorbed on gold provide similar energies for all the species, within 0.2 eV of range, being the most stable the *C1* tautomer. Table S3 in S.I. file includes the theoretical frequencies and the corresponding assignments provided from the DFT calculations. Fig. 5 shows the theoretical spectra and the optimized orientations of the four considered tautomeric forms of Cyt-d3 on gold. The closer atoms to the gold surface of tautomers *C*1, *C2* and *C4* are the oxygen (keto or enol group) and the nitrogen of the amine group. However, the keto-imino tautomer *C3* interacts with the metal by the oxygen and the intra-cyclic N1 atom. In the optimum geometries of the four adsorbed tautomers considered, the oxygen group is located *on top* of an interior gold atom of the model surface.

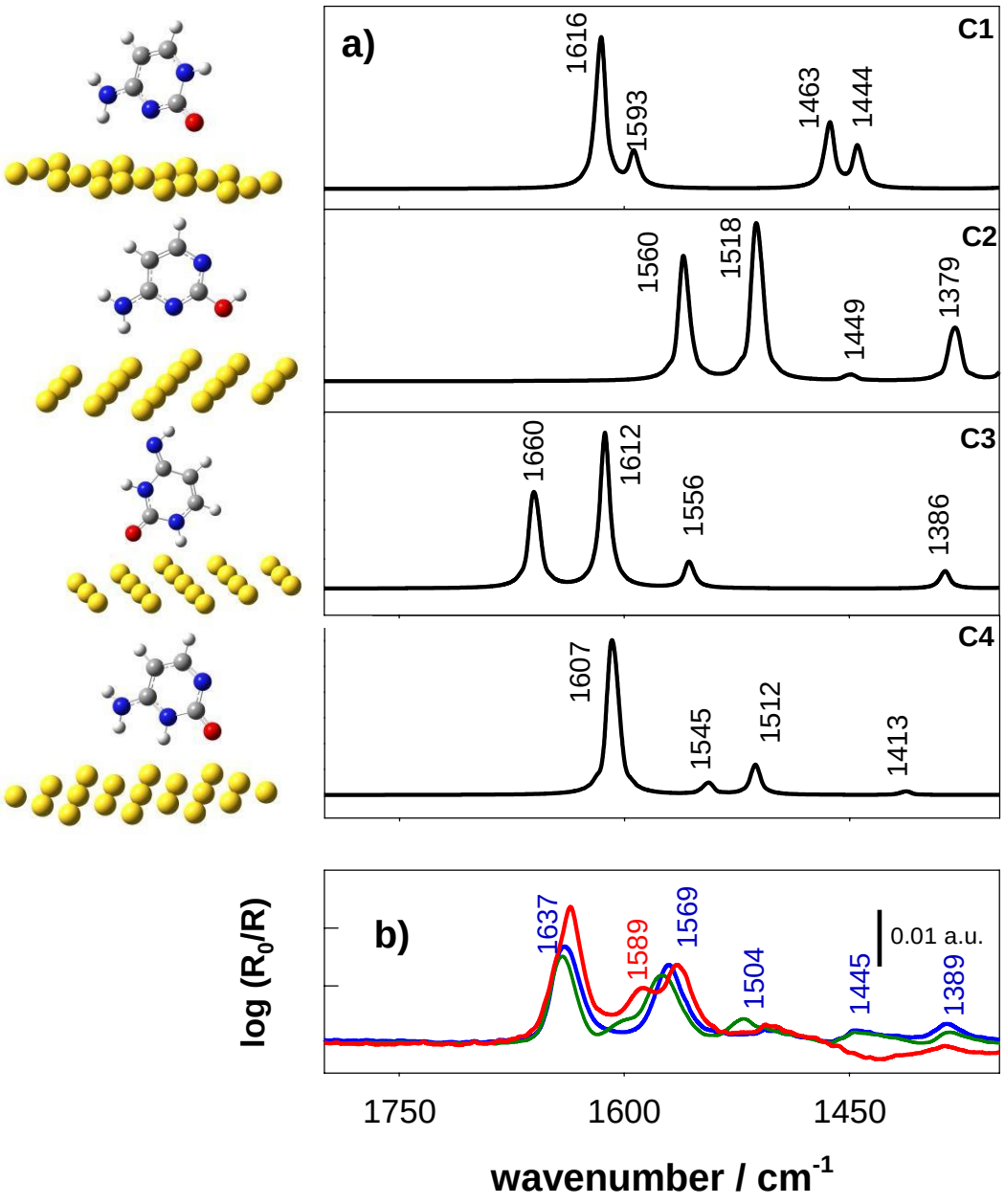

Figure 5.- a) DFT simulated IR spectra of Cyt-d3 tautomers indicated in the plots, adsorbed on gold. b) ATR-SEIRA spectra in the 1800-1350 cm^{-1} region of Cyt-d3 adsorbed on gold at the same potentials that indicated in Fig.4, from 1 mM solutions in D_2O at pD 1 (red line), 7 (blue line) and 11.8 (green line). Structures of the corresponding tautomers adsorbed on Au(111) surfaces optimized by DFT calculations are provided at the left part of the figure.

The intense band at 1637 cm^{-1} involves the presence of the carbonyl group in the adsorbed Cyt-d3 molecule, so the enol-amine tautomer *C2* can initially be disregarded as the majoritarian form. The theoretical spectrum of the *C1* tautomer provides two intense bands around 1600 cm^{-1}, compatible with the experimental results. However, it

also shows two medium intensity absorption bands at 1463 (ν_{C4C5}, δ_{CH}) and 1444 cm^{-1} (δ_{CH} ν_{C4N3}, δ_{ND2}), that do not show up in the experimental spectra. These two vibration modes around 1450 cm^{-1} of the *C1* tautomer are in plane vibration modes as the ones responsible for the signals around 1600 cm^{-1}, so they all should appear in the experimental spectrum. Therefore, *C1* tautomer, which was the majoritarian component in solution, does not contribute significantly to the spectrums of the chemisorbed adlayer. The two intense bands at 1637 and 1569 cm^{-1} can correspond to the theoretical bands at 1660 cm^{-1} (ν_{C2O}) and 1612 cm^{-1} (ν_{C5C6}, ,ν_{C4N7}, δ_{CH}) of *C3* tautomeric form. Therefore, the ATR-SEIRA spectrum of Cyt-d3 adsorbed on gold from neutral media at high potential seems to correspond to the *C3* tautomer. The same tautomeric form can explain most of the spectral features of the ATR-SEIRAS of Cyt-d3 in acid and basic media, although the additional absorption band at c.a. 1590 cm^{-1} suggests the co-existence of a different tautomer of cytosine adsorbed with *C3*, depending of the pH of the solution.

Fig. 6 shows the ATR-SEIRA spectra of Cyt-d3 as a function of the electrode potential at the three pDs considered. At pD 1, the band at 1587 cm^{-1} shows up at the lowest potentials (-0.1V) and seems to remain constant as the potential increases in the studied potential range. On the contrary, the bands at 1636 and 1563 cm^{-1} increase with the potential. A similar effect can be observed in the ATR-SEIRA spectra of Cyt-d3 adsorbed on gold from solutions at pD 11.5. In this case, the accessible potential window includes a significant potential range within the voltammetric region I, which allows one to detect a broad band around 1580 cm^{-1} that decomposes in two overlapping signals upon increasing the potential at 1600 and 1565 cm^{-1}. In the spectra at pD 8 the band at c.a. 1580 cm^{-1} is only appreciable at a limited range of potentials within the voltammetric region II. In region III the bands at 1637 and 1565 cm^{-1} increases very rapidly with potential.

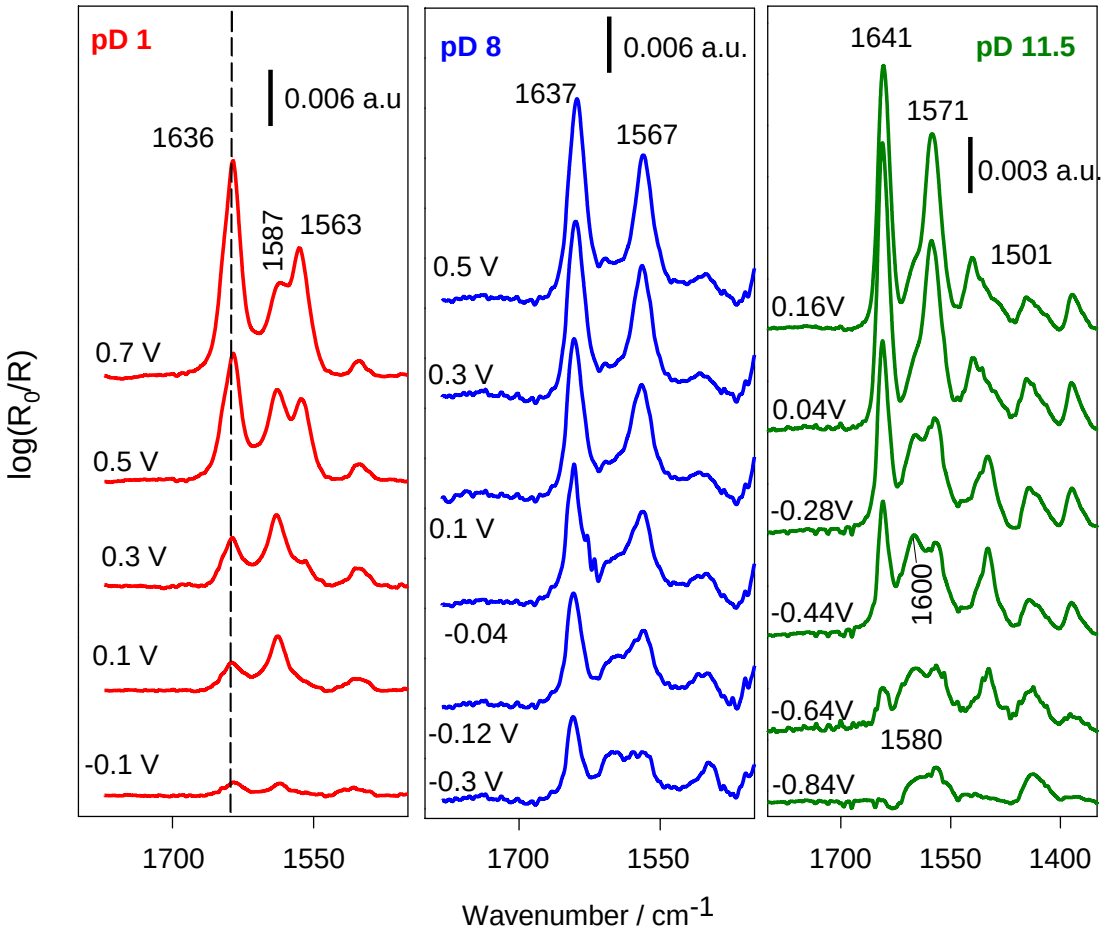

Figure 6.- ATR-SEIRA spectra in the 1800-1350 cm^{-1} region of Cyt-d3 adsorbed on gold at the indicated electrode potentials from 1 mM solutions in D_2O at pD 1 (red lines) pD 8 (blue lines) and pD 11.8 (green lines).

The spectra at every potential were deconvoluted employing Fourier-Self Deconvolution (FSD) and second derivative (SD) methodologies to reveal the sub-band structure. Then the band fitting was performed using Gaussian-Lorentzian functions for each band. In Fig 7 the deconvolution of the spectrum averaged over potentials from -0.22 to 0.5 V vs SCE in neutral media is shown as an example, in comparison to the spectra at a low and at a high potential and the spectrum of cytosine in solution. An evolution is observed as the potential is increased from the characteristics similar to the spectrum in solution to the spectra of chemisorbed cytosine. It seems at low potentials the adsorption interactions are similar to the intermolecular interactions in solution. However, the cytosine molecule is organized on the electrode with a tilted orientation that provides five surface active vibration signals in the spectral region. As the potential

is increased some of the signals become wider suggesting either stronger inter-molecular interactions or the existence of other tautomeric forms.

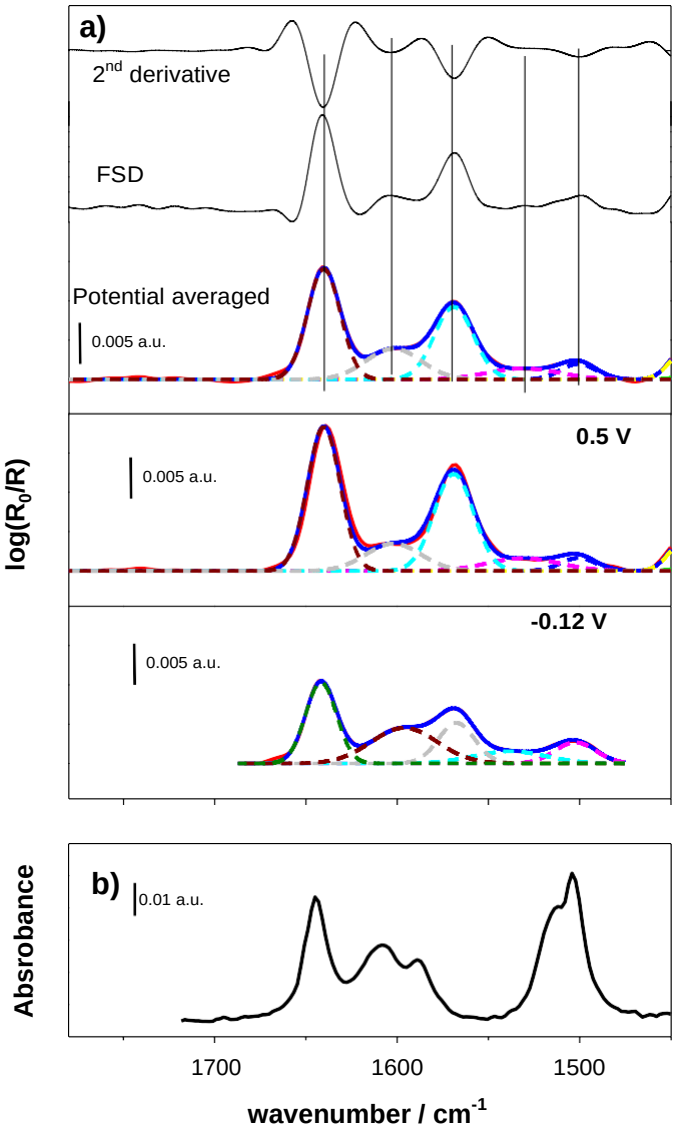

Figure 7.-a) Deconvolution of ATR-SEIRA spectra in the 1800-1350 cm^{-1} region of Cyt-d3 adsorbed on gold from 1 mM solutions in D_2O at pD 8 at the indicated electrode potentials and averaged spectrum over potential experimental range: experimental spectra (red solid lines), resulting total spectra of the deconvoluted bands (blue solid lines) and deconvoluted bands (dashed lines). The second derivative and the Fourier self-deconvolution (FSD) of the potential averaged spectrum are also included b) Transmission spectrum of Cyt-d3 10 mM in neutral solution.

The effect of the potential on the signal intensities can be more precisely observed in Fig. 8, which includes the plots of the integrated intensities of the main absorption bands (obtained in the deconvolution of the spectra) as a function of the potential.

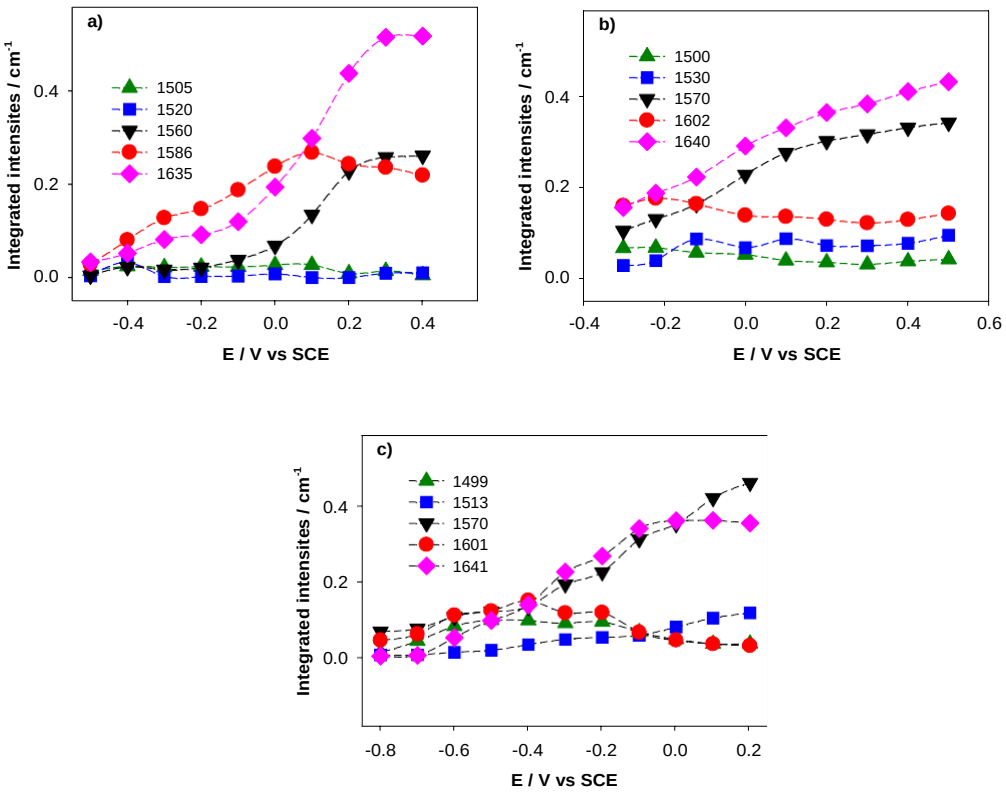

Figure 8.- Integrated intensities of the main ATR-SEIRAS absorption bands of the spectra in figure 6 as a function of the potential for Cyt-d3 adsorbed on gold from solutions of a) pD 1, b) pD 8 and c) pD 11.8.

At the three pH values considered the intensities of the bands at c.a. 1635-1641 cm^{-1} and 1563-1571 cm^{-1} increase with the potential, reaching a limiting value at potentials of the voltammetric region IV, that can be more clearly observed at pDs 8 and 11.5. This is the expected behavior for the formation of a chemically adsorbed layer, with the surface excess increasing with the potential up to a maximum value.

On the contrary, the remaining absorption bands obtained in the ATR-SEIRA spectra do not increase with the potential in the voltammetric regions II-IV, remaining nearly constant or slightly decreasing. At pD 11.5, at which the voltammetric potential region I is explored, the integrated intensities of the bands at c.a. 1590 and 1501 cm^{-1} increase with the potential up to -0.4 V, that is approximately the lowest potential of region II. Then, these integrated intensities slightly decrease with the potential. This behavior of the bands at c.a. 1590 and 1500 cm^{-1}, different from the behavior of the bands at c.a. 1635 and 1565 cm^{-1}, indicates that both set of bands correspond to different adsorbed species with different surface excess dependences with the potential and with the pH. The previous comparison in Fig. 5 between the experimental spectrum of chemisorbed

Cyt-d3 and the theoretical ones for different tautomeric forms of Cyt-d3 suggests that the majoritarian component of the adlayer in voltammetric region IV is the tautomer *C3* of cytosine. At first sight, it can be thought that a different tautomeric form is responsible for the signals at lower potentials, but none of the calculated spectra in Fig 5 for chemically adsorbed Cyt-d3 tautomers fit all the experimental observations. In fact, the experimental spectra at low potentials are closer to the spectra of deuterated cytosine, Cyt-d3, in solution, so it may be plausible that at the most negative potential regions the adsorption is not determined by the chemical interactions of the molecule with the metal atoms but to physical interactions under the electric field. In that case, the results in this potential region should be better explained by the theoretical spectra in solution, provided in Fig.2, keeping in mind that intermolecular interactions were not taken into account in the calculations. These interactions are expected to give rise to a widening of the bands. Taking this fact into account it seems that the preponderant *C1* tautomer in solution get physically adsorbed at the lower potentials, with some inclination of the molecular plane as to be able to provide surface active IR signals. However, as the region III is reached it is replaced at the interface by the chemically adsorbed *C3* tautomer.

To confirm these all hypotheses obtained from the ATR-SEIRAS of Cyt-d3 adsorbed on gold, the experimental data for adsorbed Cyt-h3 were analyzed. Fig. 9 shows the ATR-SEIRA spectra obtained for the adsorption of cytosine (Cyt-h3) on gold electrode from H_2O solutions at three different pH values and at potentials of the chemisorption region. The same main features can be observed at the three pH values consisting in four signals at c.a 1650, 1580, 1510-1515 and 1432 cm^{-1}, confirming that the same neutral cytosine get adsorbed at the three pH values. In the spectrum at pH 11.5 the bending OH mode of the solvent is not completely corrected, so Cyt-h3 signal at 1650 cm^{-1} appears at a wide band that almost overlap the cytosine band at 1581 cm^{-1}. As in the case of Cyt-d3, the comparison of the ATR-SEIRAS results with the absorption spectra of Cyt-h3 in solution reveals clear differences in the spectral features. The two intense bands obtained in ATR-SEIRAS at c.a. 1650 and 1581 cm^{-1} do not coincide with the wide band centered at 1616 cm^{-1} for Cyt-h3 in solution. On the contrary, the bands at c.a. 1504 and 1438 cm^{-1} of the spectrum of Cyt-h3 in solution can correspond to the bands in the ATR spectrum of adsorbed Cyt-h3 at 1510 and 1432 cm^{-1}.

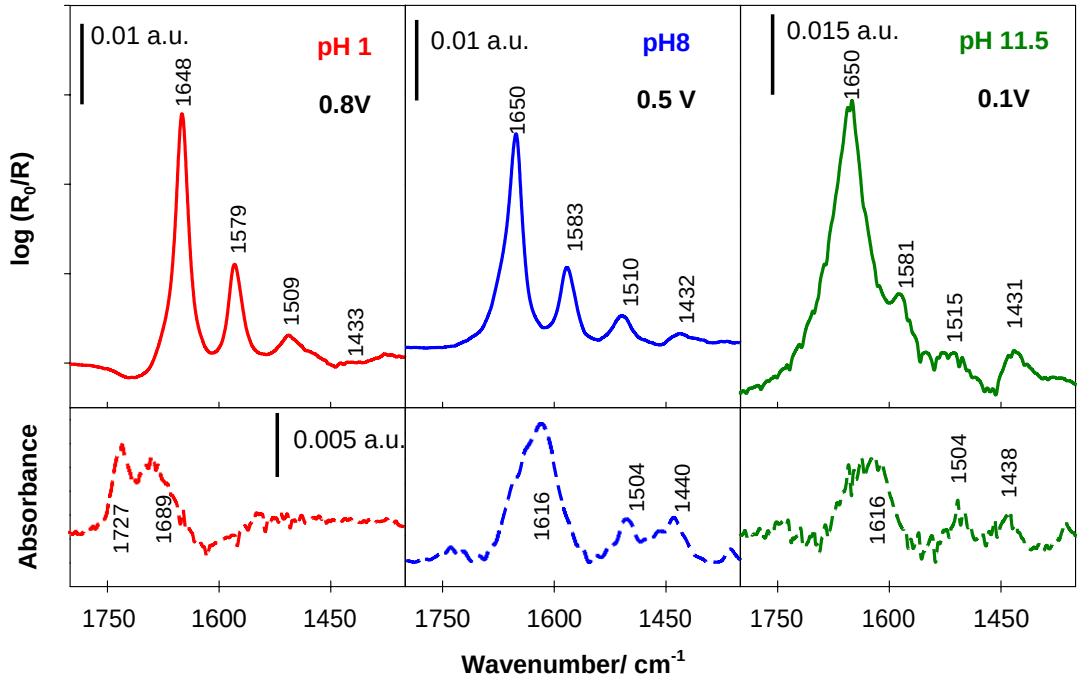

Figure 9.- ATR-SEIRA spectra of Cyt-h3 adsorbed on gold electrodes from H_2O solutions at the indicated potentials and pH values (solid lines). The absorption spectra of cytosine in solution at the same pH value are included at the lower part of the figure (dashed lines).

The influence of the electrode potential on the spectral absorption bands mentioned above can be observed in Fig. S5. There is a selective enhancement with the potential in the region II to IV of the bands at 1578 cm^{-1} and 1650 cm^{-1}. This enhancement is not present, at least in the same magnitude, in the bands at 1432 and 1510 cm^{-1}.

On the other hand, the bands at c.a. 1650 cm^{-1} and 1510 cm^{-1} shifts to the red as the potential increases, up to 16 cm^{-1} from -0.2 V to 0.8 V at pH 8. Ataka and Osawa[32] observed the same effect in the ATR-SEIRA spectra of Cyt-h3 adsorbed on gold from acid and neutral solutions. They explained this phenomenon as caused by the transition between physisorption and chemisorption of cytosine.

The ATR-SEIRA spectra of adsorbed Cyt-h3 from H_2O solutions at pH 1 and 8, in the 1400-1800 cm^{-1} region, have been deconvoluted in eight independent bands at c.a.1670, 1650, 1620, 1580, 1550, 1520, 1510 and 1450 cm^{-1}, as it is illustrated in Fig. 10. The integrated intensities of the bands at 1450, 1550 and 1620 cm^{-1} are small in the whole potential range and they are also highly dependent on the baseline correction required for the deconvolution process. The integrated intensities of the most significant bands

resulting from the deconvolution are plotted against the potential in Fig. 11. It can be observed that the band intensities of different signals have different behavior with the potential, in agreement with the work of Ataka and Osawa[32]: The band at 1670 cm^{-1} increases at very low potentials, within the voltammetric regions I and II. At higher potentials, within region III, this band decreases reaching a constant area at voltammetric region IV. On the other hand, the bands at 1580 and 1650 cm^{-1} increases in parallel with the potential in the chemisoprtion region, thus indicating that these two bands correspond to the chemically adsorbed tautomers of cytosine.

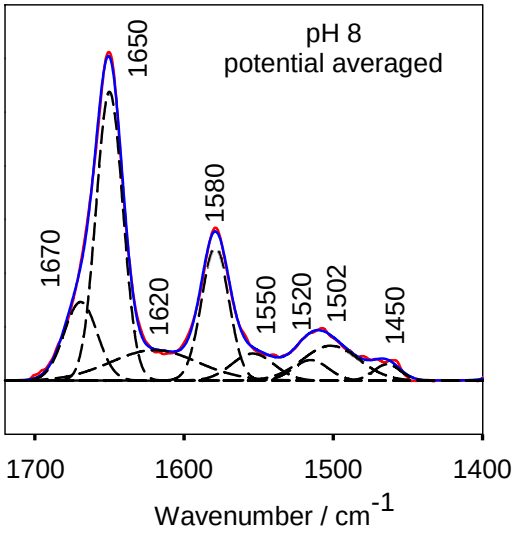

Figure 10.- Potential averaged ATR-SEIRA spectra in the 1800-1400 cm^{-1} region of Cyt-h3 adsorbed on gold from 1 mM solutions in H_2O at pH 8 (red solid line) and decovolution of the spectra in gaussian bands centered at aprox. 1450, 1502, 1520, 1550, 1580, 1620, 1650 and 1670 cm^{-1}. The sum of deconvoluted bands is also represented (blue solid line).

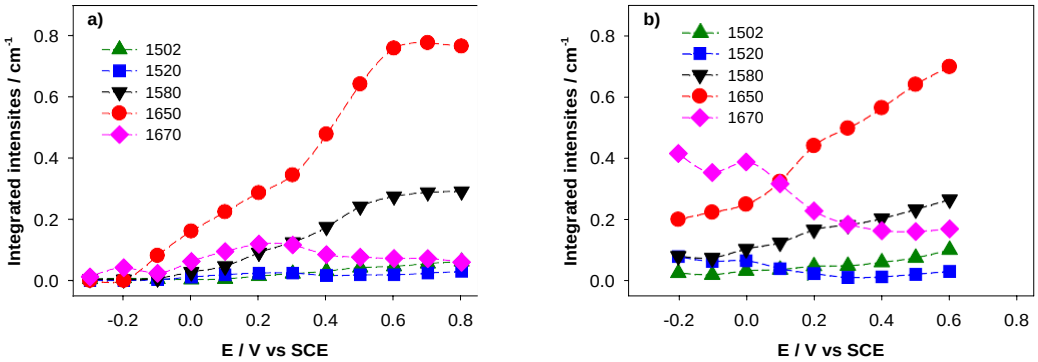

Figure 11.- Integrated intensities of the main ATR-SEIRAS absorption bands of the spectra in figure 10 as a function of the potential for Cyt-h3 adsorbed on gold from solutions of a) pH 1 and b) pH 8.

These results indicate that there are two different cytosine forms adsorbed on gold electrode, depending on the potential. The differences between both adsorbed forms can be related to the type of adsorption (physisorption or chemisorption), as suggested by Atatka and Osawa[32], but also can be related to the tautomeric equilibrium of cytosine or to both phenomena (type of adsorption and tautomeric equilibrium).

The assignments of the ATR-SEIRA bands of adsorbed Cyt-h3 from H_2O solutions to the vibrational modes of the possible cytosine tautomers has been done on the basis of DFT calculations. The theoretical frequencies corresponding to the vibrational modes of the different forms of Cyt-h3 are in table S4, and the comparison of the theoretical and experimental ATR-SEIRA spectra are shown in Figure S6. The two strong experimental ATR-SEIRA bands at 1650 and 1581 cm^{-1}, observed at a high potential (chemisorption region IV), could be explained either by the theoretical spectrum of adsorbed keto-amine cytosine tautomer *C1*, with two bands at 1637 cm^{-1} ($\nu_{CO,}$ δ_{NH2}) and 1601 cm^{-1} (ν_{C5C6}, δ_{NH2}), or by the adsorbed keto-imino *C3* tautomeric form, with bands at 1679 cm^{-1} ($\nu_{CO,}$ $\delta_{N1H,}$ δ_{N3H}) and 1625 cm^{-1} ($\nu_{C5C6,}$ $\nu_{C4N7,}$ $\delta_{N1H,}$ δ_{N3H}). However, the ATR-SEIRAS results in the region IV obtained for Cyt-d3 permitted to discard the canonical tautomer *C1* as predominant in chemically adsorbed state. Then, the keto-imine tautomer *C3* of cytosine must be responsible for the two strong bands of chemisorbed cytosine at 1650 and 1581 cm^{-1}.

However, the two very weak experimental bands at c.a. 1508 and 1440 cm^{-1}, also observed in the absorption spectra of Cyt-h3 in solution, cannot be assigned to *C3* tautomer and must be assigned to the theoretical signals of the adsorbed *C1* tautomer at 1484 cm^{-1} (ν_{C4C5}, δ_{NH}) and 1434 cm^{-1} (δ_{CH} ν_{C4N7}, δ_{NH2}), respectively. On the other hand, the experimental ATR-SEIRAS signal at 1670 cm^{-1} exhibit a potential dependence close to the potential dependence of the bands at 1434 and 1508 cm^{-1}, suggesting that the three IR bands must correspond to the same form of Cyt-h3 adsorbed on the electrode.

Therefore, the ATR-SEIRAS results for adsorbed Cyt-h3 on gold from H_2O solutions confirm that, depending on the applied potential, a different tautomeric form adsorbs on the electrode, as indicated the results obtained in D_2O. Moreover, it can be concluded that the predominant tautomer adsorbed at low potentials is the canonic keto-amine form (*C1*), probably physisorbed. The presence of active IR bands corresponding to in-plane vibrations at low potentials indicates that the pysisorbed *C1* tautomer is oriented

with the molecular plane at least tilted over the electrode surface. At higher potentials, within the chemisorption potential region, the keto-imino tautomer (*C3*) seems to be the predominant component of the ad-layer.

The potential dependence of the integrated intensities of the experimental ATR-SEIRAS bands of adsorbed cytosine depends on the surface concentration of the absorbing species and on the molecular orientation.

The integrated intensity of an ATR-SEIRA band measured with p-polarized radiation ( ) directly depends on the surface excess of the absorbing species ( ),and on the scalar product of the radiation electric field vector ( ) and the vibrational transition the dipole vector ( ):[60]

$$\propto \Gamma \times \langle \quad ^2 \rangle \cos^2(\quad) \qquad (1)$$

θ is the angle between the vector of the transition and the direction perpendicular to the metal grains reflection surface where the beam is reflected in the ATR-SEIRA set up.

The ratio between the integrated intensities of two absorption bands in the same spectral region can be considered independent on the surface excess ( ) and on the mean squared of the electric field intensity ( ):

$$\frac{}{} = \frac{^{(1)} \quad ^{(1)}}{^{(2)} \quad ^{(2)}} \frac{\cos^2(^{(1)})}{\cos^2(^{(2)})} \qquad (2)$$

Changes in this ratio with the potential must be ascribed to changes in $^{(1)}$ and $^{(2)}$, caused by reorientations of the absorbing molecule relative to the reflecting surface. In previous studies about the adsorption of adenine[45] and thymine[47] over gold electrodes it was found that both chemisorbed molecules rotate their molecular plane as the electrode potential increases. These facts were explained because of the interactions of the permanent dipole moment of the adsorbed basis and the static electric field at the interphase. The ratios between the integrated intensities of the ATR-SEIRA spectra of Cyt-d3 at c.a. 1636 and 1565 cm^{-1} (in D_2O) and between the bands at c.a. 1650 and 1580 cm^{-1} (in H_2O) do not change significantly with the potential (not

shown). Either in

D_2O and in H_2O the bands used for the ratios correspond to vibrations with transition dipole vectors with different directions within the molecular plane, so it can be concluded that the static electric field at the interphase do not affect appreciably the orientation of the adsorbed cytosine, contrary to the case of adsorbed adenine and thymine. Then, all the potential effects on the integrated intensities of the deconvoluted spectral bands have to be exclusively ascribed to changes in the surface concentrations of the absorbing species.

3.3.2.- Spectra in the 2900-3900 cm^{-1} Cyt-h3 adsorbed on gold electrodes.

In the spectral region between 2900 and 3700 cm^{-1} the absorption corresponding to OH and NH or NH_2 stretching vibrations appear so the analysis of the ATR-SEIRA spectra of adsorbed Cyt-h3 in that range of frequencies can provide extra interesting information about the adsorbed species and their orientations. Fig. 12 contains the ATR-SEIRAS results in this wavenumber range obtained for Cyt-h3 adsorbed on gold, at potentials from regions II, III and IV, in H_2O solutions at three pH values (1, 8 and 11.6).

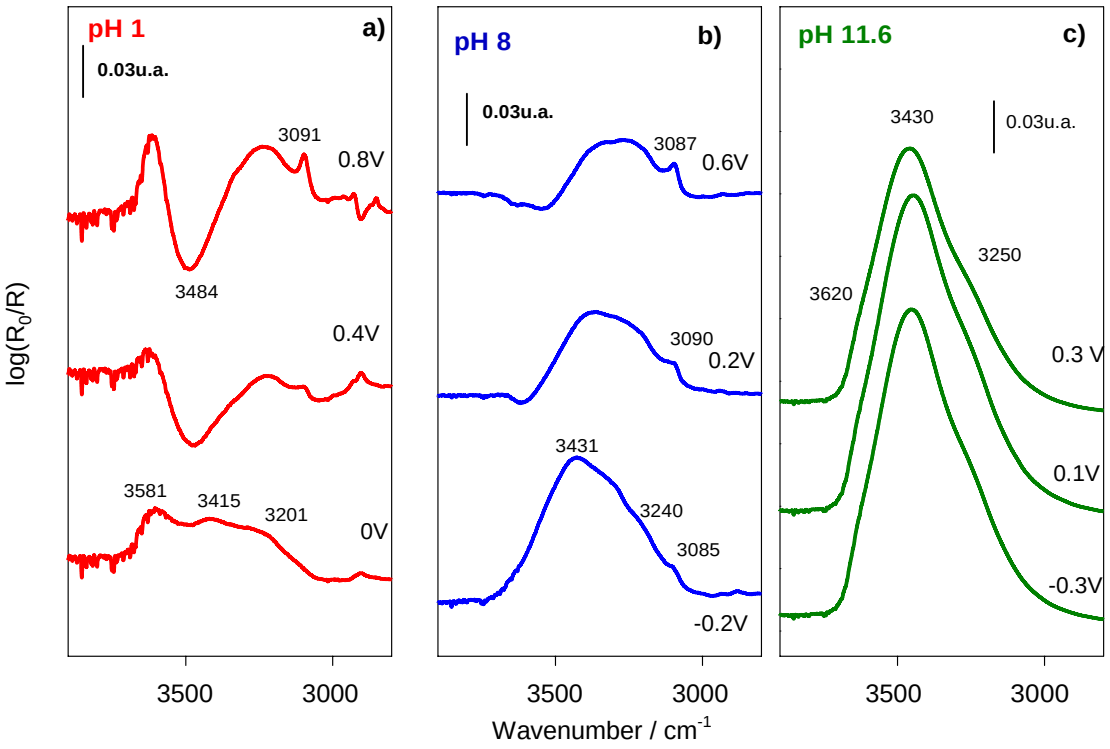

Figure 12.- .- ATR-SEIRA spectra in the 2850-3700 cm^{-1} region of Cyt-h3 adsorbed on gold from 1 mM solutions in H2O at pH 1 (red lines) pH 8 (blue lines) and pH 11.6 (green lines), at the electrode potentials indicated in the plots

The spectra obtained at pHs 11.6 and 8 show a wide and high absorption band, centered at c.a. 3430 cm^{-1} corresponding to the OH stretching (ν_{OH}) of strong, asymmetrically H-bonded water. They also include, as shoulders, the other two types of OH stretching vibrations of interfacial water oriented with the oxygen towards the electrode surface[61,62]: at c.a. 3600 cm^{-1} (ν_{OH} of non H-bonded water), and at c.a. 3250 cm^{-1} (ν_{OH} of symmetrically H-bonded water). All the spectra in this work, including those in Figure 12, are referred to the spectra registered at the same potential in the absence of Cyt-h3. Therefore, the positive absorption bands obtained in the c.a. 3600 cm^{-1} spectral region indicate an increase in the interfacial water oriented with the oxygen towards the electrode surface, either because of water co-adsorbs with Cyt-h3 or because the presence of Cyt-h3 shifts the zero charge potential to lower values, driving the reorientation of water molecules. As the potential increases the water wide band in Fig. 12 c) centered at 3430 cm^{-1} slightly decreases.

On the contrary, the ATR-SEIRA spectra obtained at pH 1 in Fig. 12 a) show the highest band at c.a. 3581 cm^{-1}. As the potential increases, the band at 3450 cm^{-1} decreases, showing negative going bands at potentials of chemisorption of adenine. These results suggest that the chemisorption of the DNA base diminishes the concentration of asymmetrically H-bonded water at the interphase.

Although the low intensity bands corresponding to NH or NH_2 stretching vibrations are overlapped by the OH stretching bands of the solvent, it is possible to observe the presence of a low and narrow band at c.a. 3090 cm^{-1} at high potentials in the ATR-SEIRA spectra of adsorbed cytosine at pH 1 and pH 8. At first sight, according to the theoretical bands for the different tautomeric forms of cytosine in Table S4 in SI, this band could correspond to the symmetric stretching of NH_2 (in the *C1*, *C2* or *C4*) tautomers or to the N1H stretching vibration in the *C3* tautomer. However, on the basis of the orientations of the cytosine tautomers over gold obtained from the DFT geometrical optimizations, given in Fig. 5, *C1*, *C2* and *C4* tautomers are oriented with the NH_2 bisector direction (coincident with the transition dipole direction) nearly parallel to the electrode surface. On the contrary, the DFT results indicate that *C3* tautomer is oriented with the N1H nearly perpendicular to the electrode. Taking into

account the surface selection rule and the low intensity of the NH or NH_2 stretching vibration bands, the small signal observed at 3090 cm^{-1} at high potentials is more likely to correspond to the N1H stretching of the *C3* tautomer form of adsorbed Cyt-h3, in good agreement with the analysis of the ATR-SEIRA spectra in the 1350-1800 cm^{-1} region.

4.- CONCLUSSIONS

The comparison of the FT-IR spectra of cytosine in solutions of D_2O and H_2O at different pH values, ranging from 1 to 11 allows us to conclude the existence of the protonated molecule at pH 1 and the neutral form at pH values higher than the pK_{a1}. The interpretations of the spectra at pH 8 and 11 on the base of DFT calculations of the spectra for different tautomers of the neutral cytosine indicate that the canonical keto-amine tautomer (*C1*) is the predominant one in solution, but the spectra show more signals in the 1600- 1500 cm^{-1} region than expected for this form. Particularly, the signal at 1587 cm^{-1} observed in the experiments in D_2O, can be better ascribed to the keto-imino tautomeric form (*C3*) than to the enol-amino form (*C2*).

The comparison of the ATR-SEIRA spectra of adsorbed cytosine at high potentials with the spectra of cytosine in solutions at the three pH values allows us to conclude that the neutral cytosine form get adsorbed even in very acid solutions. The voltametric results also indicate deprotonation phenomena associated to the adsorption in acid media. However, the ATR-SEIRA spectra show clear differences from the spectra of cytosine in solution at the same conditions, evidencing that different tautomeric forms of neutral cytosine are predominant in solution and in chemical adsorbed state. The influence of potential on the ATR-SEIRA spectra suggests also changes in the preponderance of the tautomers from the low potential region (physisorption region) to the high potential region (chemisorption region).

Interpretations of these observations have been done based on the DFT calculated spectra of adsorbed cytosine tautomers on gold clusters. These calculations indicated that all the adsorbed tautomers adopt a normal orientation of the molecular plane relative to the electrode surface, with the oxygen and amine nitrogen pointing towards the electrode, except the keto-imine form that is adsorbed with the oxygen and nitrogen

N1 towards the electrode. The experimental signals in the 1800-1350 cm-1 region of the spectra at high potentials can be explained as due to a preponderance of the chemisorbed *C3* tautomers. Thus, the two characteristic signals of the *C1* tautomer at 1463 and 1444 cm^{-1} almost disappear at the time that the bands at 1637 and 1569 cm^{-1}, that can be well assigned to the adsorbed *C3,* increases. The evolution of the spectra with potential can be explained as due to the existence of a predominant physisorbed *C1* tautomer at low potentials, providing spectral features similar to the spectra in solution, and to a predominant chemisorbed *C3* tautomer at high potentials. ATR-SEIRA spectra of cyt-h3 also confirm the evolution from the physisorbed *C1* tautomer to the chemisorbed *C3* tautomer: the bands at 1670 cm^{-1} ($\nu_{CO,}$ δ_{NH2}), 1508 (ν_{C4C5}, δ_{NH}) and 1440 cm^{-1} (δ_{CH} ν_{C4N7}, δ_{NH2}), assigned to the physically adsorbed *C1* tautomer (DFT calculated spectra of the isolated molecules) decrease, while the two strong signals at 1650 and 1581 cm^{-1}, assigned to the chemisorbed *C3* tautomer (DFT calculated spectra of the adsorbed species) increase with the potential. The small signal at 3090 cm^{-1}, due to a NH or NH_2 stretching mode, also proves the chemisorption of *C3* tautomer, as only its orientation would explain the presence of this band, according to the surface selection rules and the theoretical orientations of the adsorbed tautomers.

In addition, the ATR-SEIRA spectra of cyt-h3 in the 2900-3900 cm^{-1} show the coadsorption of water at neutral and basic pH values and the loss of H-bonded water in acid media as cytosine chemically adsorbs.

5.-ACKNOLEDGEMENTS

Financial supports from the Spanish Government (Ministry of Economy and Competitiveness - CTQ2014-57515-C2-1-R and ELECTROBIONET- CTQ2015-71955-REDT) and from the Andalusian government (PAI-FQM202) are acknowledged. Julia Álvarez-Malmagro also acknowledges a FPU grant from the Spanish Ministry of Science and Technology. The “Centro de Servicios de Informatica y Redes de Comunicaciones” (CSIRC) of the University of Granada and the general services (CITIUS) of Seville University are also acknowledged by the use of computing facilities and sputtering metalizer, respectively.

REFERENCES

[1] J.D. Watson, F.H.C. Crick, Molecular Structure of Nucleic Acids: A Structure for Deoxyribose Nucleic Acid, Nature. 171 (1953) 737–738. doi:10.1038/171737a0.

[2] J. Leszczyński, Theoretical evaluation of new nucleic acid bases. Ab initio study on tautomerism of 2,6-diaminopyrimidine (κ-base), Chem. Phys. Lett. 173 (1990) 371–377. doi:10.1016/0009-2614(90)85286-L.

[3] J. Leszczyński, Electron correlation effects in the ab initio study on tautomerism of guanine, Chem. Phys. Lett. 174 (1990) 347–354. doi:10.1016/0009-2614(90)85357-I.

[4] C. Colominas, F.J. Luque, M. Orozco, Tautomerism and protonation of guanine and cytosine. Implications in the formation of hydrogen-bonded complexes, J. Am. Chem. Soc. 118 (1996) 6811–6821. doi:10.1021/ja954293l.

[5] L. Gorb, J. Leszczynski, Intramolecular proton transfer in monohydrated tautomers of cytosine: An ab initio post-Hartree-Fock study, Int. J. Quantum Chem. 70 (1998) 855–862. doi:10.1002/(SICI)1097-461X(1998)70:4/5<855::AID-QUA31>3.0.CO;2-Y.

[6] P.Ü. Civcir, A theoretical study of tautomerism of cytosine, thymine, uracil and their 1-methyl analogues in the gas and aqueous phases using AM1 and PM3, J. Mol. Struct. THEOCHEM. 532 (2000) 157–169. doi:10.1016/S0166-1280(00)00556-X.

[7] C. Alemán, The keto–amino/enol tautomerism of cytosine in aqueous solution. A theoretical study using combined discrete/self-consistent reaction field models, Chem. Phys. 253 (2000) 13–19. doi:10.1016/S0301-0104(99)00371-7.

[8] M. Noguera, M. Sodupe, J. Bertrán, Effects of protonation on proton-transfer processes in guanine-cytosine Watson-Crick base pairs, Theor. Chem. Acc. 112 (2004) 318–326. doi:10.1007/s00214-004-0591-2.

[9] V. Zoete, M. Meuwly, Double proton transfer in the isolated and DMA-embedded guanine-cytosine base pair, J. Chem. Phys. 121 (2004) 4377–4388.

doi:10.1063/1.1774152.

[10] Y. Lin, H. Wang, S. Gao, H.F. Schaefer, Hydrogen-Bonded Proton Transfer in the Protonated Guanine-Cytosine $(GC+H)^+$ Base Pair, J. Phys. Chem. B. 115 (2011) 11746–11756. doi:10.1021/jp205403f.

[11] O.O. Brovarets, D.M. Hovorun, Why the tautomerization of the G·C Watson-Crick base pair via the DPT does not cause point mutations during DNA replication? QM and QTAIM comprehensive analysis, J. Biomol. Struct. Dyn. 32 (2014) 1474–1499. doi:10.1080/07391102.2013.822829.

[12] Y. Lin, H. Wang, Y. Wu, S. Gao, H.F. Schaefer III, Proton-transfer in hydrogenated guanine-cytosine trimer neutral species, cations, and anions embedded in B-form DNA, Phys. Chem. Chem. Phys. 16 (2014) 6717–6725. doi:10.1039/c3cp54904f.

[13] S. Tolosa, J.A. Sansón, A. Hidalgo, Mechanisms for guanine–cytosine tautomeric equilibrium in solution via steered molecular dynamic simulations, J. Mol. Liq. 251 (2018) 308–316. doi:10.1016/J.MOLLIQ.2017.12.091.

[14] J.S. Beck, J.C. Vartuli, W.J. Roth, M.E. Leonowicz, C.T. Kresge, K.D. Schmitt, C.T.W. Chu, D.H. Olson, E.W. Sheppard, S.B. McCullen, J.B. Higgins, J.L. Schlenker, A New Family of Mesoporous Molecular Sieves Prepared with Liquid Crystal Templates, J. Am. Chem. Soc. 114 (1992) 10834–10843. doi:10.1021/ja00053a020.

[15] M. Sabio, S. Topiol, W.C. Lumma, An Investigation of Tautomerism in Adenine and Guanine, J. Phys. Chem. 94 (1990) 1366–1372. doi:10.1021/j100367a032.

[16] I.R. Gould, D.V.S. Green, P. Young, I.H. Hillier, A Theoretical Study Using ab Initio Methods of Tautomerism in Cytosine in the Gas Phase and in Water, J. Org. Chem. 57 (1992) 4434–4437. doi:10.1021/jo00042a024.

[17] G. P.Ford, B. Wang, Energetics of acid-base equilibria in aqueous solution. MNDO, AMI, and PM3 results for compounds with functionalities analogous to the nucleic acids, J. Mol. Struct. THEOCHEM. 283 (1993) 49–55. doi:10.1016/0166-1280(93)87113-R.

[18] J. Florián, V. Baumruk, J. Leszczy, IR and Raman Spectra, Tautomeric Stabilities, and Scaled Quantum Mechanical Force Fields of Protonated Cytosine, (n.d.). https://pubs.acs.org/doi/pdf/10.1021/jp953284w (accessed February 8, 2018).

[19] E.L. Stewart, C.K. Foley, N.L. Allinger, J.P. Bowen, Ab initio calculations with electronic correlation (MP2) on the nucleic acid bases and their methyl derivatives, J. Am. Chem. Soc. 116 (1994) 7282–7286. doi:10.1021/ja00095a035.

[20] J. Leszczyński, Guanine, 6-thioguanine and 6-selenoguanine: ab initio HF/DZP and MP2/DZP comparative studies, J. Mol. Struct. 311 (1994) 37–44. doi:10.1016/S0022-2860(10)80012-2.

[21] I.R. Gould, N.A. Burton, R.J. Hall, I.H. Hillier, Tautomerism in uracil, cytosine and guanine: a comparison of electron correlation predicted by ab initio and density functional theory methods, J. Mol. Struct. THEOCHEM. 331 (1995) 147–154. doi:10.1016/0166-1280(94)03887-Q.

[22] J. Florian, J. Leszczynski, Spontaneous DNA mutations induced by proton transfer in the guanine.cytosine base pairs: An energetic perspective, J. Am. Chem. Soc. 118 (1996) 3010–3017. doi:10.1021/ja951983g.

[23] P. Lowdin, Proton Tunneling in DNA and tis Biological Implications, Rev. Mod. Phys. 35 (1963) 1034–1042.

[24] M.D. Topal, J.R. Fresco, Base pairing and fidelity in codon – anticodon interaction., Nature. 263 (1976) 289.

[25] L. Gorb, Y. Podolyan, P. Dziekonski, W.A. Sokalski, J. Leszczynski, Double-proton transfer in adenine-thymine and guanine-cytosine base pairs. A post-Hartree-Fock ab initio study, J. Am. Chem. Soc. 126 (2004) 10119–10129. doi:10.1021/ja049155n.

[26] K. Szczepaniak, M. Szczesniak, W. Szajda, W.B. Person, J. Leszczynski, Infrared spectra of tautomers and rotamers of 9-methylguanine. An experimental and theoretical study1, Can. J. Chem. 69 (1991) 1705–1720. doi:10.1139/v91-

251.

[27] M. Dreyfus, 0. Bensaude, G. Dodin, J. E. Dubois, Tautomerism in Cytosine and 3-Methylcytosine. A Thermodynamic and Kinetic Study, J. Am. Chem. Soc. 98 (1976) 6338–6349. doi:10.1021/ja00436a045.

[28] M.J. Nowak, K. Szczepaniak, Infrared matrix isolation studies on tautomerism of cytosine and isocytosine methyl-derivatives, J. Mol. Struct. 115 (1984) 221–224. doi:10.1016/0022-2860(84)80054-X.

[29] M. Szczesniak, J. Leszczyiiski, W.B. Person, Identification of the Imino-oxo form of 1-methylcytosine, J. Am. Chem. Soc. 114 (1992) 2731–2733.

[30] R. Otero, W. Xu, M. Lukas, R.E.A. Kelly, E. Laegsgaard, I. Stensgaard, J. Kjems, L.N. Kantorovich, F. Besenbacher, Specificity of Watson-Crick Base Pairing on a Solid Surface Studied at the Atomic Scale, Angew. Chemie Int. Ed. 47 (2008) 9673–9676. doi:10.1002/anie.200803333.

[31] S. Liu, G. Zheng, J. Li, Raman spectral study of metal-cytosine complexes: A density functional theoretical (DFT) approach, Spectrochim. Acta - Part A Mol. Biomol. Spectrosc. 79 (2011) 1739–1746. doi:10.1016/j.saa.2011.05.049.

[32] K. Ataka, M. Osawa, In situ infrared study of cytosine adsorption on gold electrodes, J. Electroanal. Chem. 460 (1999) 188–196. doi:10.1016/S0022-0728(98)00375-1.

[33] J. Lipkowski, Building biomimetic membrane at a gold electrode surface., Phys. Chem. Chem. Phys. 12 (2010) 13874–13887. doi:10.1039/c0cp00658k.

[34] K.Y. Wong, B.M. Pettitt, A study of DNA tethered to a surface by an all-atom molecular dynamics simulation, Theor. Chem. Acc. 106 (2001) 233–235. doi:10.1007/s002140100269.

[35] H. Cohen, C. Nogues, R. Naaman, D. Porath, Direct measurement of electrical transport through single DNA molecules of complex sequence, in: Proc. Natl. Acad. Sci., 2005: pp. 11589–11593.

[36] D. Porath, A. Bezryadin, S. De Vries, C. Dekker, Direct measurement of

electrical transport through DNA molecules, Nature. 403(6770) (2000) 635.

[37] B.Q. Xu, P.M. Zhang, X.L. Li, N.J. Tao., Direct Conductance Measurement of Single DNA Molecules in Aqueous Solution, Nano Lett. 4 (2004) 1105–1108. doi:10.1103/PhysRevA.92.052113.

[38] T. Wandlowski, D. Lampner, S.M. Lindsay, Structure and stability of cytosine adlayers on Au(111): an in-situ STM study, J. Electroanal. Chem. 404 (1996) 215–226. doi:10.1016/0022-0728(95)04235-0.

[39] N.J. Tao, J.A. De Rose, S.M. Lindsay, Self-Assembly of Molecular Superstructures Studied by in situ Scanning Tunneling Microscopy: DNA bases on Au(111), J Phys Chem. 97 (1993) 910–919. doi:10.1021/j100106a017.

[40] H. Farrokhpour, H. Jouypazadeh, Description of adenine and cytosine on Au(111) nano surface using different DFT functionals (PW91PW91, wB97XD, M06-2X, M06-L and CAM-B3LYP) in the framework of ONIOM scheme: Non-periodic calculations, Chem. Phys. 488–489 (2017) 1–10. doi:10.1016/J.CHEMPHYS.2017.03.001.

[41] M. Rosa, W. Sun, R. Di Felice, Interaction of DNA Bases with Gold Substrates, J. Self-Assembly Mol. Electron. 1 (2013) 41–68. doi:10.13052/same2245-4551.112.

[42] J. Alvarez-Malmagro, M. Rueda, F. Prieto, In situ surface-enhanced infrared spectroscopy study of adenine-thymine co-adsorption on gold electrodes as a function of the pH, J. Electroanal. Chem. 819 (2018) 417–427. doi:/doi.org/10.1016/j.jelechem.2017.11.054.

[43] J. Álvarez-Malmagro, F. Prieto, M. Rueda, A. Rodes, In situ Fourier transform infrared reflection absorption spectroscopy study of adenine adsorption on gold electrodes in basic media, Electrochim. Acta. 140 (2014) 476–481. doi:10.1016/j.electacta.2014.03.074.

[44] M. Rueda, F. Prieto, A. Rodes, J.M. Delgado, In situ infrared study of adenine adsorption on gold electrodes in acid media, Electrochim. Acta. 82 (2012) 534–542. doi:10.1016/j.electacta.2012.03.070.

[45] F. Prieto, Z. Su, J.J. Leitch, M. Rueda, J. Lipkowski, Quantitative Subtractively Normalized Interfacial Fourier Transform Infrared Reflection Spectroscopy Study of the Adsorption of Adenine on Au(111) Electrodes, Langmuir. 32 (2016) 3827–3835. doi:10.1021/acs.langmuir.6b00635.

[46] M. Rueda, F. Prieto, J. Álvarez-malmagro, A. Rodes, Evidences of adenine – thymine Interactions at gold electrodes interfaces as provided by in-situ infrared spectroscopy, Electrochem. Commun. 35 (2013) 53–56. doi:10.1016/j.elecom.2013.07.026.

[47] F. Prieto, J. Alvarez-Malmagro, M. Rueda, J.M. Orts, Tautomerism of adsorbed Thymine on gold electrodes: an in situ surface-enhanced infrared spectroscopy study, Electrochim. Acta. 201 (2016) 300–310. doi:10.1016/j.electacta.2015.11.109.

[48] R.M.C. Dawson, Data for biochemical research, Clarendon Press, 1989. https://global.oup.com/academic/product/data-for-biochemical-research-9780198552994?cc=ca&lang=en& (accessed November 6, 2018).

[49] Clavilier J, Flame-Annealing and Cleaning Tecnique, in: A. Wieckowski (Ed.), Interfacial Electrochem. Theory Exp. Appl., CRC, 1999: pp. 231–248.

[50] J. Clavilier, R. Faure, G. Guinet, R. Durand, Preparation of monocrystalline Pt microelectrodes and electrochemical study of the plane surfaces cut in the direction of the {111} and {110} planes, J. Electroanal. Chem. Interfacial Electrochem. 107 (1980) 205–209. doi:10.1016/S0022-0728(79)80022-4.

[51] A. Berná, J.M. Delgado, J.M. Orts, A. Rodes, J.M. Feliu, In-situ infrared study of the adsorption and oxidation of oxalic acid at single-crystal and thin-film gold electrodes: A combined external reflection infrared and ATR-SEIRAS approach, Langmuir. 22 (2006) 7192–7202. doi:10.1021/la060400l.

[52] D.A. Skoog, F.J. Holler, S.R. Crouch, Principles of instrumental analysis, 7th ed., Cengage Learning, Boston, 2017.

[53] M.J. Frisch, G.W. Trucks, H.B. Schlegel, G.E. Scuseria, M.A. Robb, J.R. Cheeseman, G. Scalmani, V. Barone, B. Mennucci, G.A. Petersson, H. Nakatsuji,

M. Caricato, X. Li, H.P. Hratchian, A.F. Izmaylov, J. Bloino, G. Zheng, D.J. Sonnenb, Gaussian 09, (2016).

[54] W.J. Hehre, R. Ditchfield, J.A. Pople, Self—Consistent Molecular Orbital Methods. XII. Further Extensions of Gaussian—Type Basis Sets for Use in Molecular Orbital Studies of Organic Molecules, J. Chem. Phys. 56 (1972) 2257–2261. doi:10.1063/1.1677527.

[55] T. Clark, J. Chandrasekhar, G.W. Spitznagel, P.V.R. Schleyer, Efficient diffuse function-augmented basis sets for anion calculations. III. The 3-21+G basis set for first-row elements, Li-F, J. Comput. Chem. 4 (1983) 294–301. doi:10.1002/jcc.540040303.

[56] P.C. Hariharan, J.A. Pople, The influence of polarization functions on molecular orbital hydrogenation energies, Theor. Chim. Acta. 28 (1973) 213–222. doi:10.1007/BF00533485.

[57] I.M. Alecu, J. Zheng, Y. Zhao, D.G. Truhlar, Computational Thermochemistry: Scale Factor Databases and Scale Factors for Vibrational Frequencies Obtained from Electronic Model Chemistries, J. Chem. Theory Comput. 6 (2010) 2872–2887. doi:10.1021/ct100326h.

[58] P.J. Hay, W.R. Wadt, *Ab initio* effective core potentials for molecular calculations. Potentials for K to Au including the outermost core orbitals, J. Chem. Phys. 82 (1985) 299–310. doi:10.1063/1.448975.

[59] W. Haiss, B. Roelfs, S.N. Port, E. Bunge, H. Baumgartel, R.J. Nichols, In-situ infrared spectroscopic studies of thymine adsorption on a Au(111) electrode, J. Electroanal. Chem. 454 (1998) 107–113. doi:10.1016/s0022-0728(98)00243-5.

[60] M. Osawa, Surface-Enhanced Infrared Absorption, in: S. Kawata (Ed.), Top. Appl. Phys., Springer, 2001: pp. 163–187. doi:10.1007/3-540-44552-8_9.

[61] K. Ataka, T. Yotsuyanagi, M. Osawa, Potential-Dependent Reorientation of Water Molecules at an Electrode/Electrolyte Interface Studied by Surface-Enhanced Infrared Absorption Spectroscopy, J. Phys. Chem. 100 (1996) 10664–10672. http://pubs.acs.org/doi/abs/10.1021/jp953636z (accessed April 5, 2017).

[62] K. Ataka, M. Osawa, In Situ Infrared Study of Water−Sulfate Coadsorption on Gold(111) in Sulfuric Acid Solutions, Langmuir. 14 (1998) 951–959. doi:10.1021/la971110v.